

Original Article

Application of natural and synthetic goethite for the removal
of methylene blue from aqueous solutionsNasir Abdus-Salam¹, Fabian Audu Ugbe^{2*}, and Victoria Abiola Ikudayisi-Ugbe¹¹ Faculty of Physical Sciences, Department of Chemistry, University of Ilorin, Ilorin, Nigeria² Faculty of Physical Sciences, Department of Chemistry, Ahmadu Bello University, Zaria, Nigeria

Received: 6 July 2020; Revised: 20 August 2021; Accepted: 6 September 2021

Abstract

Unregulated discharge of untreated effluents into the environment by industries constitutes one of the major sources of pollution. Adsorption technique was since discovered as a highly efficient and cheap technique for effluent detoxification. The search for an efficient, low-cost, and readily available adsorbent necessitated this study, which investigates the sorption of methylene blue (MB) from aqueous solution by natural goethite (NGT) and synthetic goethite (SGT) particles using batch equilibrium technique. The effects of initial concentration, NGT particle size, adsorbent dosage and solution pH were evaluated, and found to have remarkable influence on the adsorption processes with optimum (pH of 12, concentration of 200 mg/L for MB-NGT, 250 mg/L for MB-SGT and 0.112 mm mesh for NGT). The adsorption characteristics were quite similar, though with the adsorption capacities of 1.826 mg/g (NGT) and 27.322 mg/g (SGT). Results of isotherm modeling revealed the order of fittings; Langmuir ($R^2 = 0.9727$) > Freundlich (0.9323) > Temkin (0.8113) for MB-NGT and Temkin (0.9217) > Freundlich (0.9171) > Langmuir (0.8529) for MB-SGT. An evaluation of isotherm investigation results with those of the kinetics and thermodynamic study (Ugbe & Abdus-Salam, 2020), suggest a combined physisorption and chemisorption mechanism. Therefore, this study provides useful information on the application of both goethite forms for MB removal.

Keywords: adsorption, natural goethite, synthetic goethite, methylene blue, isotherms**1. Introduction**

One of the major challenges regarding many industries, especially the textile industry and dyeing activities is the release of large volume of colored effluent from their production process into the environment (Othmana *et al.*, 2018). This causes damage to the quality of receiving streams and other water bodies and is also toxic to food chain organisms (Agalya, Palanisamy & Sivakumar, 2012). Treatment of this dye effluent constitutes a significant environmental challenge as most dyes have very complex molecular structures which enhance their non-biodegradability when released into the environment (Zargar, Parham & Rezazade, 2011). The cationic dye, methylene blue (MB) has

a wide application in wood, silk, leather and cotton processing, which perhaps accounts for its availability in industrial wastewater (Luo *et al.*, 2019). MB (Figure 1) is an organic chloride salt with the formula $C_{16}H_{18}ClN_3S$, molecular weight of 319.85 g/mol, melting point of 100 to 110 °C and soluble in glycerol, water, chloroform, glacial acetic acid, and ethanol (Utsev, Iwar & Ifyale, 2020). In aqueous solutions, it exists as $[C_{16}H_{18}N_3S]^+$ (Fangwen *et al.*, 2009). MB releases certain aromatic amines such as benzidine, methylene, and others, and as such being potentially carcinogen (Moorthy, Rathi, Shukla, Kumar & Bharti, 2021). Methylene blue was recently reported to cause severe central nervous system toxicity (Gillman, 2011). Toxicity of MB not only arrests the growth of photoautotrophic organisms such as microalgae but also leads to reduced oxygenation of water due to inhibition of photosynthesis (Moorthy *et al.*, 2021).

Several techniques are developed and used for the treatment of dye effluents, such as freeze-casting of alumina

*Corresponding author

Email address: ugbefabianaudu@gmail.com

ultra-filtration membranes with good performance for anionic dye separation (Liu, Zhu, Guan, Peng & Wu, 2018); efficient activation of peroxymonosulfate by porous Co-doped LaFeO₃ for organic pollutants degradation in water (Ji, Xie, Zheng & Xu, 2021a); and microbial decolorization of textile dye containing effluents, a review (Banat, Nigam, Singh & Marchant, 1996). Amongst others are removal of ionic dyes from water by solvent extraction using reverse micelles (Pandit & Basu, 2004), and adsorption of anionic dyes from aqueous solutions by calcined and uncalcined mg/al layered double hydroxide (Siti, Zaini & Nesamalar, 2016). Adsorption is one of the most popular methods amongst these, especially using waste materials as the adsorbent(s) because of their low cost, high efficiency and ease of handling (Anirudhan & Rejeena, 2015).

Goethite is an iron mineral bearing hydroxy group which enables it to bind strongly to both organic and inorganic ligands (Liu, Chen & Frost, 2013). Goethite particles show high specific surface areas and strong affinities for surface binding of ions (Wang, Chen & Zhang, 2019). Synthesized goethite when compared with their naturally occurring counterparts has an improved purity and tailored composition with desired particle size, surface properties and color (Nayak & Rao, 2005). In this study, alpha goethite (α -FeOOH) was used.

Some researchers have earlier investigated the adsorption properties of locally available materials for methylene blue removal such as Pumice stone (Derakhshan *et al.*, 2013), potassium hydroxide treated *metroxylon spp.* (Amode, Santos, Alam, Mirza & Mei, 2016), activated carbon/iron oxide nanoparticle (Zargar *et al.*, 2011), magnetic chitosan composite (Jumadi *et al.*, 2019), dry polymer beads (Yadav *et al.*, 2020), activated carbon from biowaste of fir bark (Luo *et al.*, 2019), surfactant modified activated carbon (Kuang, Zhang & Zhou, 2020), biochar/Fe_xO_y composite (Zhanga *et al.*, 2020), and poly (pyrrole methane) based adsorbent (Ji, Zhang, Yang, Ma & Xu, 2021b), amongst others.

The continuous search for suitable adsorbent for the removal of dye from effluents, plus the harmful nature of concentrated dye led to the choice of MB as a model compound for evaluating the potentials of natural goethite (NGT) and synthetic goethite (SGT) for its removal from wastewaters. Moreover, there are only a few instances in literature where goethite was applied in the treatment of dye effluents, such as; Congo red on calcium alginate beads impregnated with nano-goethite (Munagapati & Kim, 2017) and MB on goethite nano adsorbents (Nassar & Ringsred, 2012).

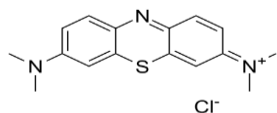


Figure 1. Chemical structure of MB

2. Materials and Methods

2.1 Preparation of adsorbents

Sample of SGT (α -FeOOH) used in this study was synthesized in the laboratory according to the method reported

by Lee, Kim, Choi and Huh (2004), while the NGT sample was collected from the National Iron Ore Mining Company (NIOMCO), Itakpe, Kogi State, Nigeria. Both Samples were then prepared and characterized using X-ray fluorescence (XRF, SHIMADZU model), Fourier transform infrared spectroscopy (FTIR, SHIMADZU), scanning electron microscope (SEM, SHIMADZU), Brunauer–Emmett–Teller (BET) specific surface area (NOVA STATION C), and nano-sizing (MALVERN), as published elsewhere by Abdus-Salam, Ugbe and Funtua (2018), who also reported the result of point of zero charge (pHpzc) experiment conducted on both adsorbents.

2.2 Adsorption experiment

Batch technique was used to investigate the effect of different parameters such as initial solution concentration, adsorbent particle size, adsorbent load and pH on the uptake of MB by NGT and SGT. A 15 ml solution of varying concentrations (5, 10, 50, 100, 150, 200, 250, 300 and 400) ppm MB were added to 0.5 g of NGT (different particle sizes; 0.112 mm, 0.25 mm and 0.50 mm) and 0.1g SGT in separate conical flasks of 100 ml capacity and mechanically agitated on an orbital conical flask shaker for 2 hrs at 27 °C. At the end of the reaction, the solutions were then filtered and the resulting filtrates analyzed for MB concentration using UV-visible spectrophotometer (SHIMADZU series) at a known wavelength of maximum absorption (Abdus-Salam & Adekola, 2005). Note that NGT was studied at varying particle sizes because different sieve sizes were used during the size reduction process, and as such it became necessary to investigate the adsorption capacity as a function of particle size. SGT however was synthesized as fine particles and therefore was not subjected to size reduction.

The optimum concentration obtained was then used as the working concentration in the subsequent experiment carried out to examine the effect of initial solution pH (2, 3, 4, 5, 6, 7, 8, 10 and 12) and adsorbent dosage (0.05, 0.1, 0.15, 0.20, 0.25 and 0.5) g. The amounts of dye adsorbed at equilibrium were determined using equation 1 (Ibrahim & Jimoh, 2008).

$$q_e = \frac{V(C_i - C_e)}{m} \quad (1)$$

where q_e is MB concentration (mg/g) removed by the adsorbent at equilibrium, v is the initial volume of dye solution (L), C_i and C_e is the initial concentration and equilibrium concentration of MB in the solution (mg/L) respectively, while m is adsorbent load (g). Experimental results were fitted into three common isotherm models; Langmuir, Freundlich and Temkin as given by the equations in Table 1 (Behbahani & Behbahani, 2014; Temkin & Pyozhev, 1940; Zelentsov, Datsko & Dvornikova, 2012). The experiment for the effects of contact time (kinetic study) and temperature (thermodynamic study) was earlier conducted with the results published by Ugbe and Abdus-Salam (2020).

3. Results and Discussion

3.1 Effect of initial solution concentration

The result of the adsorption of MB onto NGT and

Table 1. Some adsorption isotherm equations and their parameters

Isotherm	Equation	Parameters	Equation no.
Langmuir	$\frac{C_e}{q_e} = \frac{1}{q_m} C_e + \frac{1}{K_a q_m}$	Plot: C_e/q_e versus C_e q_e = ads capacity (mg.g ⁻¹) q_m = max ads capacity (mg.g ⁻¹) C_e = equil conc (mgL ⁻¹) K_a = Reation constant describing affinity (L/mg)	2
Freundlich	$\log q_e = \log K_F + \frac{1}{n} \log C_e$	Plot: $\log q_e$ versus $\log C_e$ n = ads intensity K_F = Reaction constant reflecting ads capacity (L/mg)	3
Temkin	$q_e = B \ln A + B \ln C_e$ $B = \frac{RT}{b}$	Plot: q_e versus $\ln C_e$ A = equil ads constant (L/mg) b = Temkin isotherm constant relating to heat of ads (J/mol) R = 8.314 J/molK T = Absolute temp (K)	4

ads = adsorption, equil. = equilibrium, temp = temperature, max = maximum, conc. = concentration

SGT at varying initial solution concentration is presented in Figure 2.

From Figure 2, the quantity of MB sorbed onto both goethite forms increased with initial solution concentrations until reaching 200 mg/L for MB-NGT and 250 mg/L for MB-SGT, before the adsorption then falls slightly. This trend may be as a result of the saturation of the adsorption sites of NGT and SGT at higher concentrations. SGT relatively exhibited greater adsorption capacity for MB removal and at higher concentration regardless of its small mass of 0.10 g compared to the 0.50 g NGT used. This may be due to the fact that SGT, an iron compound contains relatively higher percent of pure goethite particles. Hence, sorption sites of SGT tend to reach saturation only at higher concentration. This observation is in conformity with the result reported by Abdus-Salam and Adekola (2005).

3.2 Effect of variation of natural goethite particle size

The result of the adsorption of MB by NGT at varying particle sizes (0.112, 0.25 and 0.50) mm is presented in Figure 3.

The study showed that uptake of MB is dependent on the size of NGT particles as observed from Figure 3. Amongst the various particle sizes tested, 0.112 mm of NGT demonstrated the greatest maximum adsorption capacity for uptake of MB followed closely by 0.25 mm particle. The difference in the quantity of adsorbed MB became even wider as the initial solution concentration increases. The observed decrease in the adsorption capacity with increasing particle size can be attributed to a relatively large surface area exhibited by the smaller particle sizes of NGT. For the larger particle size adsorbent, there is a relatively greater diffusional resistance to mass transport making the accessibility or utilization of the internal surface of these particles difficult. Similar result was obtained by Ugbe, Funtua & Ikudayisi (2018).

3.3 Effect of variation of adsorbent dosage

The result of the adsorption of MB onto NGT and SGT at varying dosages (0.05, 1.0, 0.15, 0.20, 0.25 and 0.5) g is given in Figure 4.

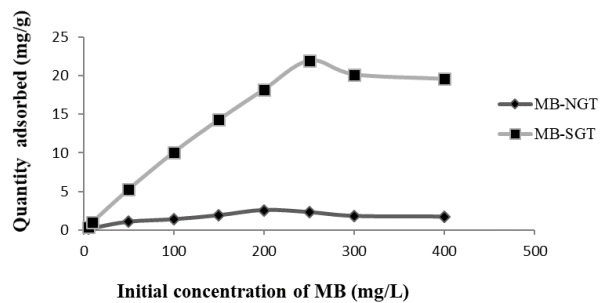


Figure 2. Effect of initial concentration on the adsorption of MB on NGT and SGT

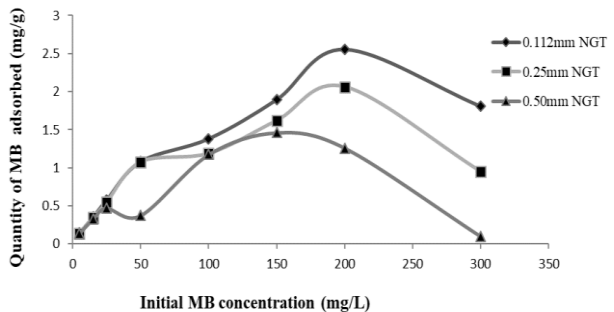


Figure 3. Effect of variation of particle size on MB adsorption at varying concentration

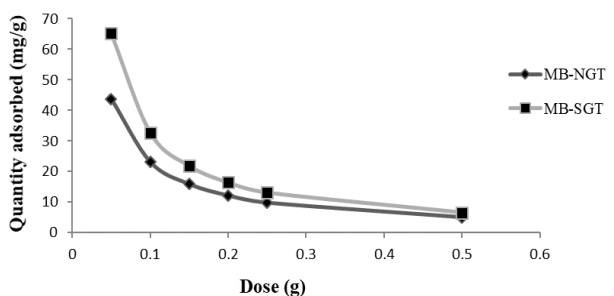


Figure 4. Effect of variation of adsorbent dosage on sorption of MB onto NGT and SGT

The declining curve of quantity adsorbed (mg/g) against adsorbent load (Figure 4) indicates a decrease in the adsorption capacity of both adsorbents as their dosage increases. This may be as a result of the overlapping or aggregation of sorption sites of the adsorbents at higher dosage, which gives rise to a decrease in useful surface area of the adsorbents, and increase the path length over which the adsorbate may diffuse or travel to reach an available sorption site. Similar result was obtained elsewhere by Crini and Badot (2008).

3.4 Effect of initial solution pH

The quantity of MB adsorbed in mg/g plotted against the initial pH is shown in Figure 5.

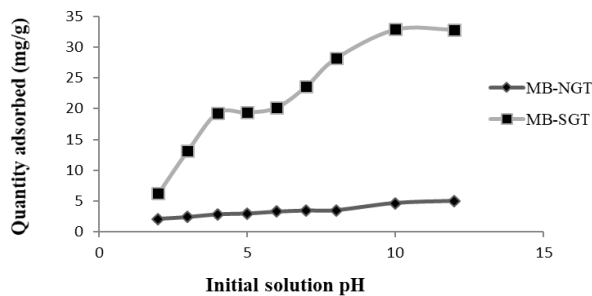


Figure 5. Effect of Initial solution pH on the sorption of MB onto NGT and SGT

Figure 5 showed that as solution pH increase from 2 to 12, the quantities of MB adsorbed increased correspondingly from 2.119 mg/g to 5.024 mg/g for MB-NGT and 6.215 mg/g to 32.84 mg/g for MB-SGT. The surface characteristics of goethite depend greatly on the pH of the solution and vary between $=\text{FeOH}_2^+$, $=\text{FeOH}$ and $=\text{FeO}^-$ as follows (Nguyen, Pham & Nguyen, 2019):



At acidic pH (pH lower than $\text{pH}_{\text{pzc}} = 6.9$ for NGT and $\text{pH}_{\text{pzc}} = 8$ for SGT) as earlier reported by Abdus-Salam *et al.* (2018), equation (2) predominates while equation (3) is for higher pH (pH greater than $\text{pH}_{\text{pzc}} = 6.9$ for NGT and $\text{pH}_{\text{pzc}} = 8$ for SGT). Chemical adsorption of MB on goethite surface happened either by the surface ligand complex reaction and/or via hydrogen bond formation (Fangwen *et al.*, 2009). The lower adsorption of MB at acidic pH was probably due to the presence of excess H^+ ions which tend to compete with the dye cation for adsorption sites. At higher pH however, the surface of both goethite particles become negatively charged as result of presence of FeO^- , which perhaps enhances the binding of positively charged dye cations via electrostatic forces of attraction (equation 4). It may also be by hydrogen bond formation between the Nitrogen atoms of MB and OH group of goethite, though the surface ligand complex reaction predominates at higher solution pH.



Similar result was obtained for MB on Iron-Oxide Coated Porous Ceramic Filter (IOCPCF) by Fangwen *et al.* (2009).

3.5 Adsorption isotherm study

Table 2 shows the linearized isotherm parameters as calculated from the isotherm equations while the various isotherm plots are presented in Figures 6 to 8.

Various values of correlation coefficient (R^2) as shown in Table 2 are in the order; Langmuir > Freundlich > Temkin for MB-NGT and Temkin > Freundlich > Langmuir for MB-SGT.

The good fits to Langmuir isotherm showed that adsorption of MB onto NGT may follow monolayer coverage, with uniform adsorption energies across the surface. This however may not hold as the values of the separation factor, R_L shown in Table 2 indicates unfavorable adsorption of MB onto NGT (i.e. $R_L > 1$). This may be attributed to the surface characteristics and chemical composition of the goethite obtained from natural deposit (NGT). Also, the values of the maximum adsorption capacity (q_m) and that obtained experimentally (q_{exp}) are only fairly close for both adsorbents. This suggests that the adsorbate (MB) accessibility to the active sites of the adsorbents may be restricted, non-uniformity of binding energies and that the sorption process may not be monolayer regardless of high R^2 values. Similar observation was reported by Abdus-Salam and Adekola (2005).

The Freundlich exponent, n , should have values in the range of 1 to 10 for adsorption to be termed as favorable adsorption. Isotherms with n greater than 1 show a high affinity between adsorbate and adsorbent and reflective of chemisorptions (Taha, Ahmad, Aziz & Chik, 2009). As seen from Table 2, the values of n all are greater than 1, meaning a high affinity between MB and both adsorbents, and which depicts chemisorptions. Therefore, the goodness of fits of Freundlich model suggests that the adsorption of MB onto both adsorbents may proceed by multilayer adsorption on already chemisorbed layer. This is in conformity with results earlier reported by Shahryari, Goharrizi and Azadi (2010).

Table 2. Adsorption isotherm parameters for the sorption of MB onto NGT and SGT

Parameters	MB-NGT	MB-SGT
Langmuir Isotherm		
R^2	0.9727	0.8529
K_L (L/g)	0.702	0.014
q_{exp} (mg/g)	2.555	21.95
q_m (mg/g)	1.826	27.322
R_L	7.072	0.222
Freundlich Isotherm		
R^2	0.9323	0.9171
K_F	0.303	0.388
n	2.682	1.214
Temkin Isotherm		
R^2	0.8113	0.9217
A (L/mg)	5.376	0.376
B (J/mol)	0.287	4.811
b_0 (J/mol)	8777.5	523.62

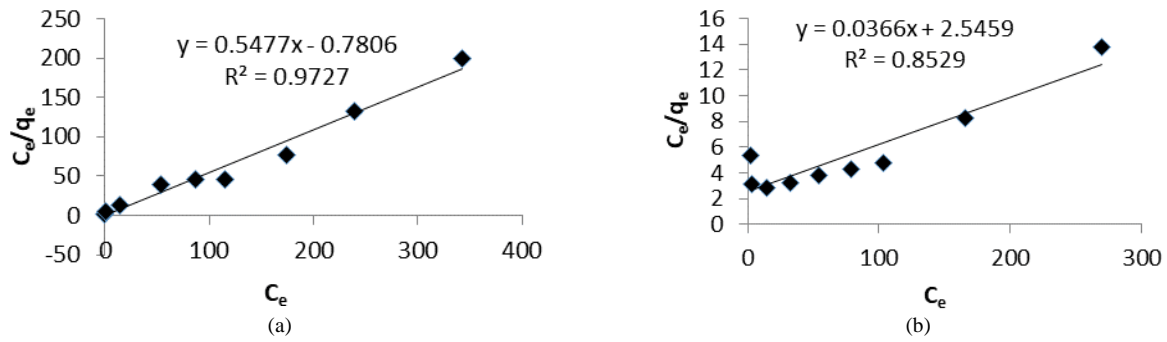


Figure 6. Langmuir isotherm plots for (a) MB-NGT (b) MB-SGT

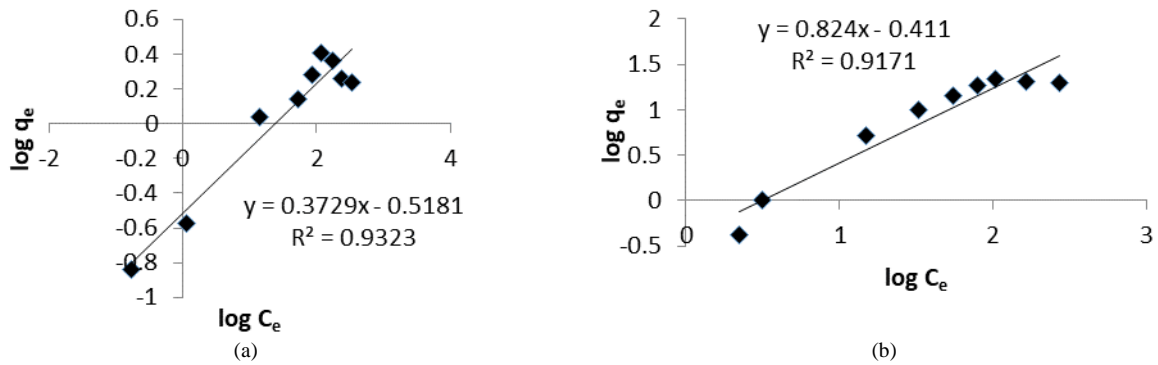


Figure 7. Freundlich isotherm plots for (a) MB-NGT (b) MB-SGT

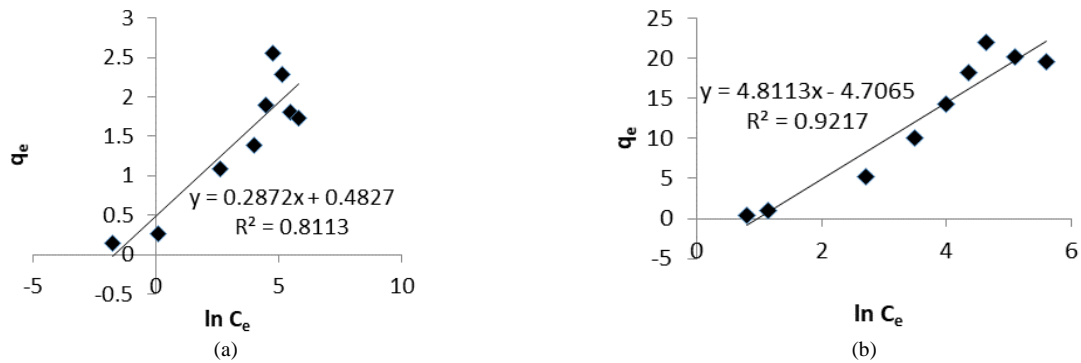


Figure 8. Temkin isotherm plots for (a) MB-NGT (b) MB-SGT

Linear plots for adsorption data into Temkin adsorption isotherm with good R^2 value consider the process as chemisorption of an adsorbate onto the adsorbent (Boparai, Joseph & O'Carroll, 2010). The goodness of fit of Temkin isotherm further supports the findings that the adsorption of MB onto both goethite surfaces may involve a chemisorptions process as suggested by the Freundlich isotherm model. This is in agreement with results obtained by Shahryari *et al.* (2010). Furthermore, the Temkin constant (b_0) which has to do with the heat of adsorption and linearly decreases as the adsorbent surface is been filled owing to interaction between analyte and adsorbent is given as 8777.5 J/mol for MB-NGT and 523.62 J/mol for MB-SGT. The lower value reported for SGT indicates a greater interaction between it and MB, suggesting a decrease in the heat of adsorption of all molecules in the layer (Ugbe *et al.*, 2018).

Also, the results of the kinetic and thermodynamic study earlier conducted on same adsorbate and adsorbents by Ugbe and Abdus-Salam (2020), showed that adsorption of MB onto both adsorbents may have proceeded through chemisorptions as revealed by the sorption kinetics, while the magnitudes of ΔH and ΔH_r suggest greatly some element of physisorption. Therefore, the combined results of isotherm, kinetics and thermodynamic studies of the adsorption of MB onto both adsorbents suggest an element of combined physisorption and chemisorption mechanism. Table 3 compares the adsorption isotherm parameters obtained for sorption of MB by other adsorbents with those obtained in this study.

4. Conclusions

This study was conducted in furtherance of the

Table 3. Comparison of some isotherm parameters (q_e , n and b_0) for methylene blue on different adsorbent materials

Adsorbent	Isotherm parameters			Author (s)
	q_e (mg/g)	n	b_0 (J/mol)	
Pumice stone	15.87	2.18	712.63	Derakhshan <i>et al.</i> , 2013
KOH treated <i>metroxylon spp.</i>	212.8	-	-	Amode <i>et al.</i> , 2016
AC/iron oxide nanoparticle	47.62	2.60	-	Zargar <i>et al.</i> , 2011
Magnetic chitosan composite	0.1308	2.43	-	Jumadi <i>et al.</i> , 2019
Dry polymer beads	10.638	1.60	-	Yadav <i>et al.</i> , 2020
AC from biowaste of fir bark	1044.4	1.32	-	Luo <i>et al.</i> , 2019
Surfactant modified AC	232.5	3.14	-	Kuang <i>et al.</i> , 2020
Biochar/Fe ₃ O ₄ composite	562	1.92	-	Zhanga <i>et al.</i> , 2020
NGT	1.826	2.68	8777.5	present study
SGT	27.322	1.21	523.62	present study

AC = Activated carbon

search for an efficient, low-cost and readily available adsorbent to investigate the sorption of methylene blue (MB) from aqueous solution by natural goethite (NGT) and synthetic goethite (SGT) particles using the batch equilibrium technique. The results of the study have shown that uptake of MB by both adsorbents is dependent on the initial solution concentration, adsorbent dosage and initial solution pH. The adsorption capacities of NGT and SGT are 1.826 mg/g and 27.322 mg/g respectively. The experimental data fitted well tested isotherm models in the order; Langmuir > Freundlich > Temkin for MB-NGT and Temkin > Freundlich > Langmuir for MB-SGT. The favourability of the adsorption process was however revealed by the obtained Freundlich and Temkin isotherm parameters for both adsorbents, suggesting chemisorptions. Therefore, the earlier results of kinetics and thermodynamic study (Ugbe & Abdus-Salam, 2020) together with that of isotherm study suggest that the adsorption process may be via a combined physisorption and chemisorption mechanism.

It can therefore be concluded that the two goethite forms can be applied for the removal of MB from aqueous solution with the synthetic goethite having relatively higher adsorption efficiency.

References

- Abdus-Salam, N., & Adekola, F. A. (2005). Physico-chemical characterization of some Nigerian goethite mineral samples. *Ife Journal of Science*, 7(1), 131 – 137.
- Abdus-Salam, N., Ugbe, F. A., & Funtua, M. A. (2018). Characterization of synthesized goethite and natural goethite sourced from Itakpe in North Central, Nigeria. *ChemSearch Journal*, 9(2), 24 – 32.
- Agalya, A., Palanisamy, P. N. & Sivakumar, P. (2012). Kinetics, equilibrium studies on removal of ionic dyes using a novel non-conventional activated carbon. *International Journal of Chemistry Research*, 3(1), 62-68.
- Amode, J. O., Santos, J. H., Alam, Z. M., Mirza, A. H., & Mei, C. C. (2016). Adsorption of methylene blue from aqueous solution using untreated and treated (*Metroxylon spp.*) waste adsorbent: Equilibrium and kinetics studies, *International Journal of Industrial Chemistry*, 7, 333– 345.
- Anirudhan, T. S., & Rejeena, S. R. (2015). Photocatalytic degradation of eosin yellow using poly (pyrrole-co-aniline)-coated TiO₂/nanocellulose composite under solar light irradiation. *Journal of Materials*, 2015. doi:10.1155/2015/636409.
- Banat, I. M., Nigam, P., Singh, D. & Marchant, R. (1996). Microbial decolorization of textile-dyecontaining effluents: A review. *Bioresource Technology*, 58 (3), 217- 227.
- Behbahani, J. T. & Behbahani, J. Z. (2014). A new study on asphaltene adsorption in porous media. *Petroleum and Coal*, 56(5), 459-466.
- Boparai, H. K., Joseph, M. & O'Carroll, D. M. (2010). Kinetics and thermodynamics of cadmium ion removal by adsorption onto nano zerovalent iron particles. *Journal of Hazardous Materials*, 186(1), 458-465.
- Crini, G. & Badot, P. M. (2008). Application of chitosan, a natural aminopolysaccharide, for dye removal from aqueous solutions by adsorption processes using batch studies: A review of recent literature. *Progress in Polymer Science*, 33(4), 399-447.
- Derakhshan, Z., Baghapour, M.A., Ranjbar, M., Baghapour, M. A., Ranjbar, M., & Faramarziyan, M. (2013). Adsorption of methylene blue dye from aqueous solutions by modified pumice stone: Kinetics and Equilibrium Studies. *Health Scope*, 2(3), 136–44.
- Fangwen, L. I., Xiaoai, W. U., Songjiang, M. A., Zhongjian, X. U., Wenhua, L. I. U. & Fen, L. I. U. (2009). Adsorption and desorption mechanisms of methylene blue removal with iron-oxide coated porous ceramic filter. *Water Resource and Protection*, 1, 1-57.
- Gillman, P. K. (2011). CNS toxicity involving methylene blue: the exemplar for understanding and predicting drug interactions that precipitate serotonin toxicity. *Journal of Psychopharmacology*, 25(3), 429-36.
- Ibrahim, M. B., & Jimoh, W. L. O. (2008). Adsorption studies for the removal of Cr (VI) ion from aqueous solution. *Bayero Journal of Pure and Applied Sciences*, 1(1), 99 – 103.
- Ji, Y., Xie, Y., Zheng, L. & Xu, F. (2021a). Efficient activation of peroxymonosulfate by porous Co-doped LaFeO₃ for organic pollutants degradation in

- water. *Journal of Solid State Chemistry*, 297, 122077.
- Ji, Y., Zhang, W., Yang, H., Ma, F. & Xu, F. (2021b). Green synthesis of poly (pyrrole methane) for enhanced adsorption of anionic and cationic dyes from aqueous solution. *Journal of Colloid and Interface Science*, 590, 396-406.
- Jumadi, J., Kamari, A., Rahim, N. A., Wong, S. T. S., Yusoff, S. N. M., Ishak, S., Abdulrasool, M. M., Kumaran, S. (2019). Removal of methylene blue and Congo red by magnetic chitosan nanocomposite: Characterization and adsorption studies. *Journal of Physics: Conference Series*, 1397(1) 012027.
- Kuang, Y. Zhang, X., & Zhou, S. (2020). Adsorption of methylene blue in water onto activated carbon by surfactant modification. *Water*, 12, 587, 1-19.
- Lee, G. H. Kim, S. H. Choi, B. J., & Huh, S. H. (2004). Magnetic properties of needle-like α -FeOOH and γ -FeOOH nanoparticles. *Journal of the Korean Physical Society*, 45(4), 1019-1024.
- Liu, H., Chen, T. & Frost, R. L. (2013). An overview of the role of goethite surfaces in the environment. *Chemosphere*, 103, 1–11.
- Liu, Y., Zhu, W., Guan, K., Peng, C. & Wu, J. (2018). Freeze-casting of alumina ultra-filtration membranes with good performance for anionic dye separation. *Ceramics International*, 44(10), 11901-11904.
- Luo, L., Wu, X., Li, Z., Zhou, Y., Chen, T., Fan, M., & Zhao, W. (2019). Synthesis of activated carbon from biowaste of fir bark for methylene blue removal. *Royal Society Open Science*, 6, 190523.
- Moorthy, A. B., Rathi, B. G., Shukla, S. P., Kumar, K. & Bharti, V. S. (2021). Acute toxicity of textile dye Methylene blue on growth and metabolism of selected freshwater microalgae. *Environmental Toxicology and Pharmacology*, 82, 103552.
- Munagapati, V. S. & Kim, D. (2017). Equilibrium isotherms, kinetics, and thermodynamic studies for congo red adsorption using calcium alginate beads impregnated with nano-goethite. *Ecotoxicology and Environmental Safety*, 141, 226-234.
- Nassar, N. N. & Ringsred, A. (2012). Rapid adsorption of methylene blue from aqueous solutions by goethite nano adsorbents. *Environmental Engineering Science*, 29(8), 790-797.
- Nayak, R., & Rao, J. R. (2005). Synthesis of active goethite and maghemite from scrap iron sources. *Journal of Scientific and Industrial Research*, 64, 35 – 40.
- Nguyen, D. V., Pham, P. T. & Nguyen, T. H. (2019). Feasibility of goethite nanoparticles for Pb(II) and Cd(II) removal from aqueous solution. *Vietnam Journal of Chemistry*, 57(3), 281-287.
- Othmana, N. H., Alias, N. H., Shahruddina, M. Z., Bakara, N. F. A., Hima, N. R. N., & Laub, W. J. (2018). Adsorption kinetics of methylene blue dyes onto magnetic graphene oxide. *Journal of Environmental Chemical Engineering*, 6, 2803–2811.
- Pandit, P. & Basu, S. (2004). Removal of ionic dyes from water by solvent extraction using reverse micelles. *Environmental Science and Technology*, 38(8), 2435–2442.
- Shahryari, Z., Goharrizi, A. S., & Azadi, M. (2010). Experimental study of methylene blue adsorption from aqueous solutions onto carbon nano tubes. *International Journal of Water Resources and Environmental Engineering*, 2(2), 016-028.
- Siti, S. M., Zaini, H. & Nesamalar, K. (2016). Adsorption of anionic dyes from aqueous solutions by calcined and uncalcined mg/al layered double hydroxide. *Malaysian Journal of Analytical Sciences*, 20(4), 777 – 792.
- Taha, M. R., Ahmad, K., Aziz, A. A. & Chik, Z. (2009). Geo-environmental aspects of tropical residual soils. In B. B. K. Huat, G. S. Sew, & F. H. Ali (Eds.), *Tropical Residual Soils Engineering* (pp. 377-403). London, England: A.A. Balkema
- Temkin, M. J. & Pyozhev, V. (1940). Kinetics of ammonia synthesis on promoted iron catalyst. *Acta Physicochimica U.R.S.S.*, 12, 327-352.
- Ugbe, F. A. & Abdus-Salam, N. (2020). Kinetics and thermodynamic modelling of natural and synthetic goethite for dyes scavenging from aqueous systems. *Arabian Journal of Chemical and Environmental Research*, 7(1), 12–28.
- Ugbe, F. A., Funtua, M. A., & Ikudayisi, V. A. (2018). Adsorption isotherms and thermodynamics study of Cd (II), Cr (III) and Cr (VI) binding by natural goethite and synthetic goethite adsorbents. *Nigerian Journal of Chemical Research*, 23(2), 1-19.
- Utsev, J. T., Iwar, R. T. & Ifyalem, K. J. (2020). Adsorption of methylene blue from aqueous solution onto *Delonix regia* pod activated carbon: batch equilibrium isotherm, kinetic and thermodynamic studies. *Journal of Materials and Environmental Science*, 11(7), 1058-1078.
- Wang, X., Chen, N., & Zhang, L. (2019). Enhanced Cr (VI) immobilization on goethite derived from an extremely acidic environment. *Environmental Science: Nano*, 6, 2185 – 2194.
- Yadav, S., Asthana, A., Chakraborty, R., Jain, B., Singh, A. K., Carabineiro, S. A. C., & Susan, M. H. (2020). Cationic dye removal using novel magnetic/activated charcoal/ β -cyclodextrin/alginate polymer Nanocomposite. *Nanomaterials*, 10, 170.
- Zargar, B., Parham, H., & Rezazade, M. (2011). Fast removal and recovery of methylene blue by activated carbon modified with magnetic iron oxide nanoparticles. *Journal of the Chinese Chemical Society*, 58, 694-699.
- Zelentsov, V., Datsko, T., & Dvornikova, E. (2012). Adsorption models for treatment of experimental data on removal of fluorine from water by oxihydroxides of aluminum. *Romai Journal*, 8(1), 209–215.
- Zhanga, P., Connora, D., Wang, Y., Jiang, L., Xiab, T., Wang, L., Tsangc, D. C. W., Okd, Y. S. & Houa, D. (2020). A green biochar/iron oxide composite for methylene blue removal. *Journal of Hazardous Materials*, 384, 121286.